Research Article | Vol. 26, No. 15 | 23 Jul 2018 | OPTICS EXPRESS 19470
Optics EXPRESS

Antireflection self-reference method based on ultrathin metallic nanofilms for improving terahertz reflection spectroscopy

WEIEN LAI,[1,*] HAIBING CAO,[1] JUN YANG,[1] GUANGSHENG DENG,[1] ZHIPING YIN,[1] QIAN ZHANG,[2] BEATRIZ PELAZ,[3] AND PABLO DEL PINO[3]

[1]*National Engineering Laboratory of Special Display Technology, National Key Laboratory of Advanced Display Technology, Academy of Photoelectric Technology, HeFei University of Technology, HeFei, 230009, China*
[2]*Institute of Nano Biomedicine and Engineering, Shanghai Engineering Research Center for Intelligent Diagnosis and Treatment Instrument, Key Laboratory for Thin Film and Microfabrication Technology of the Ministry of Education, Department of Instrument Science and Engineering, School of Electronic Information and Electrical Engineering, Shanghai Jiao Tong University, 800 Dongchuan RD, Shanghai 200240, China*
[3]*Centro Singular de Investigación en Química Biolóxica e Materiais Moleculares (CIQUS), Departamento de Física de Partículas, Universidade de Santiago de Compostela, Santiago de Compostela 15782, Spain*
**wnlai@hfut.edu.cn*

Abstract: We present the potential of an antireflection self-reference method based on ultrathin tantalum nitride (TaN) nanofilms for improving terahertz (THz) reflection spectroscopy. The antireflection self-reference method is proposed to eliminate mutual interference caused by unwanted reflections, which significantly interferes with the important reflection from the actual sample in THz reflection measurement. The antireflection self-reference model was investigated using a wave-impedance matching approach, and the theoretical model was verified in experimental studies. We experimentally demonstrated this antireflection self-reference method can completely eliminate the effect of mutual interference, accurately recover the actual sample's reflection and improve THz reflection spectroscopy. Our method paves the way to implement a straightforward, accurate and efficient approach to investigate THz properties of the liquids and biological samples.

OCIS codes: (310.1210) Antireflection coatings; (300.6495) Spectroscopy, terahertz.

References and links

1. B. Ferguson and X. C. Zhang, "Materials for terahertz science and technology," Nat. Mater. **1**(1), 26–33 (2002).
2. M. Tonouchi, "Cutting-edge terahertz technology," Nat. Photonics **1**(2), 97–105 (2007).
3. D. G. Cooke, F. A. Hegmann, E. C. Young, and T. Tiedje, "Electron mobility in dilute GaAs bismide and nitride alloys measured by time-resolved terahertz spectroscopy," Appl. Phys. Lett. **89**(12), 122103 (2006).
4. P. U. Jepsen, D. G. Cooke, and M. Koch, "Terahertz spectroscopy and imaging–Modern techniques and applications," Laser Photonics Rev. **5**(1), 124–166 (2011).
5. E. Pickwell, B. E. Cole, A. J. Fitzgerald, M. Pepper, and V. P. Wallace, "In vivo study of human skin using pulsed terahertz radiation," Phys. Med. Biol. **49**(9), 1595–1607 (2004).
6. U. Møller, D. G. Cooke, K. Tanaka, and P. U. Jepsen, "Terahertz reflection spectroscopy of Debye relaxation in polar liquids," J. Opt. Soc. Am. B **26**(9), A113–A125 (2009).
7. J. Shi, Y. Wang, T. Chen, D. Xu, H. Zhao, L. Chen, C. Yan, L. Tang, Y. He, H. Feng, and J. Yao, "Automatic evaluation of traumatic brain injury based on terahertz imaging with machine learning," Opt. Express **26**(5), 6371–6381 (2018).
8. W. E. Lai, H. W. Zhang, Y. H. Zhu, and Q. Y. Wen, "A novel method of terahertz spectroscopy and imaging in reflection geometry," Appl. Spectrosc. **67**(1), 36–39 (2013).
9. W. Withayachumnankul, J. F. O'Hara, W. Cao, I. Al-Naib, and W. Zhang, "Limitation in thin-film sensing with transmission-mode terahertz time-domain spectroscopy," Opt. Express **22**(1), 972–986 (2014).
10. P. U. Jepsen, U. Møller, and H. Merbold, "Investigation of aqueous alcohol and sugar solutions with reflection terahertz time-domain spectroscopy," Opt. Express **15**(22), 14717–14737 (2007).

#330282 https://doi.org/10.1364/OE.26.019470
Journal © 2018 Received 7 May 2018; revised 10 Jul 2018; accepted 11 Jul 2018; published 18 Jul 2018

Optics EXPRESS

11. P. C. Ashworth, E. Pickwell-MacPherson, E. Provenzano, S. E. Pinder, A. D. Purushotham, M. Pepper, and V. P. Wallace, "Terahertz pulsed spectroscopy of freshly excised human breast cancer," Opt. Express **17**(15), 12444–12454 (2009).
12. R. M. Woodward, B. E. Cole, V. P. Wallace, R. J. Pye, D. D. Arnone, E. H. Linfield, and M. Pepper, "Terahertz pulse imaging in reflection geometry of human skin cancer and skin tissue," Phys. Med. Biol. **47**(21), 3853–3863 (2002).
13. C. Rønne and S. R. Keiding, "Low frequency spectroscopy of liquid water using THz-time domain spectroscopy," J. Mol. Liq. **101**(1-3), 199–218 (2002).
14. S. Y. Huang, Y. X. Wang, D. K. Yeung, A. T. Ahuja, Y. T. Zhang, and E. Pickwell-Macpherson, "Tissue characterization using terahertz pulsed imaging in reflection geometry," Phys. Med. Biol. **54**(1), 149–160 (2009).
15. M. Nagai, H. Yada, T. Arikawa, and K. Tanaka, "Terahertz time-domain attenuated total reflection spectroscopy in water and biological solution," Int. J. Infrared Millim. Waves **27**(4), 505–515 (2006).
16. S. Huang, P. C. Ashworth, K. W. Kan, Y. Chen, V. P. Wallace, Y. T. Zhang, and E. Pickwell-MacPherson, "Improved sample characterization in terahertz reflection imaging and spectroscopy," Opt. Express **17**(5), 3848–3854 (2009).
17. M. Dressel and G. Grüner, "Electrodynamics of solids: optical properties of electrons in matter," (AAPT, 2002).
18. A. Thoman, A. Kern, H. Helm, and M. Walther, "Nanostructured gold films as broadband terahertz antireflection coatings," Phys. Rev. B **77**(19), 195405 (2008).
19. W. E. Lai, H. W. Zhang, Y. H. Zhu, Q. Y. Wen, W. W. Du, and X. L. Tang, "Bilayer metallic nanofilms as broadband antireflection coatings in terahertz optical systems," Opt. Express **22**(3), 2174–2184 (2014).
20. W. Lai, N. Born, L. M. Schneider, A. Rahimi-Iman, J. C. Balzer, and M. Koch, "Broadband antireflection coating for optimized terahertz beam splitters," Opt. Mater. Express **5**(12), 2812–2819 (2015).
21. J. Kröll, J. Darmo, and K. Unterrainer, "Metallic wave-impedance matching layers for broadband terahertz optical systems," Opt. Express **15**(11), 6552–6560 (2007).
22. M. Born and E. Wolf, Principles of Optics (Pergamon Press 1980).
23. C. Brückner, T. Käsebier, B. Pradarutti, S. Riehemann, G. Notni, E.-B. Kley, and A. Tünnermann, "Broadband antireflective structures applied to high resistive float zone silicon in the THz spectral range," Opt. Express **17**(5), 3063–3077 (2009).
24. S. McKnight, K. Stewart, H. Drew, and K. Moorjani, "Wavelength-independent anti-interference coating for the far-infrared," Infrared Phys. **27**(5), 327–333 (1987).
25. E. Pickwell, B. Cole, A. Fitzgerald, V. Wallace, and M. Pepper, "Simulation of terahertz pulse propagation in biological systems," Appl. Phys. Lett. **84**(12), 2190–2192 (2004).
26. J. Kindt and C. Schmuttenmaer, "Far-infrared dielectric properties of polar liquids probed by femtosecond terahertz pulse spectroscopy," J. Phys. Chem. **100**(24), 10373–10379 (1996).
27. J. Barthel, K. Bachhuber, R. Buchner, and H. Hetzenauer, "Dielectric spectra of some common solvents in the microwave region. Water and lower alcohols," Chem. Phys. Lett. **165**(4), 369–373 (1990).

1. Introduction

Terahertz radiation lies between microwave and infrared radiation, which is within the frequency range for macromolecule's vibration and rotational frequencies. The terahertz radiation possesses a unique property for noninvasive spectroscopy and imaging of materials [1,2]. Terahertz spectroscopy and imaging are potential tools to nondestructively probe both chemical and structural information of materials [3], such as liquids and biomaterials [4–6]. Terahertz time-domain spectroscopy (THz-TDs) has been shown to be an important technique for studying liquids and biomaterials, and probing drugs-of-abuse and explosives [7,8]. THz-TDs is suitable for determining complex refractive index and dielectric function of materials, which is difficult to be obtained by traditional optical spectrometers [9].

To study terahertz properties of liquids and biological samples, terahertz measurements of liquids and biological samples were usually performed by THz-TDs in reflection geometry [10]. Due to strict requirements of sample preparation and the need of a special holder [11], it is difficult to perform the terahertz measurement of liquids and biological samples in transmission geometry. Moreover, most of liquids and biological samples have strong absorption of THz radiation, so that the sample measurement performed in the transmission geometry is limited. For terahertz measurements of liquids and biological samples, the reflection geometry is more feasible than transmission geometry [12]. In the terahertz measurement of reflection geometry, the liquids and biological samples are typically placed on a substrate, which is made of materials with negligible absorption in the terahertz frequency range, such as high-resistivity silicon and z-cut quartz. As a result, THz detector in the THz reflection measurement receives THz superposed reflection signals from the lower

Optics EXPRESS

and upper surfaces of the substrate, as shown in Fig. 1(b). This phenomenon was called mutual interference. It arises from the ring tail (unwanted reflection) of the reference reflection from the lower surface of the substrate, which significantly interferes with the sample reflection from the upper surface of the substrate. The mutual interference influences the accuracy of sample information in the THz reflection measurement. Thus, in order to accurately acquire sample information, we need to eliminate mutual interference and to recover the reflection from the actual sample in the reflection measurement. However, the conventional method in the THz reflection measurement generally uses a thicker substrate of higher refractive index (such as silicon) to provide a greater optical delay between the reference reflection (from the lower surface of the substrate) and the sample reflection (from the upper surface of the substrate) [12–14]. Since the ringing tail of the reference reflection has further to propagate before it interferes with the sample reflection, the ringing tail is likely to be weaker. But, it has still an influence on accurate sample characterization. In addition, various methods for the THz reflection measurement of liquids and biological samples was proposed, including the ATR(attenuated total reflectance) method [15], the sample baseline method [16] and the optical delay method based on a thicker substrate [13]. However, these methods can partly reduce the effect of mutual interference but cannot completely eliminate the effect and have complicated measurement requirements, which restrict their practical applications.

In this paper, an antireflection (AR) self-reference method based on ultra-thin TaN nanofilms is proposed to eliminate mutual interference, to accurately recover the sample reflection and to improve the THz measurement of liquids and biological samples. This method paves the way to implement an accurate, easy and efficient route to investigate THz properties of liquids and biological samples. In addition, the apparent advantages of TaN nanofilms, such as low-cost, present high-stability and environmental compatibility, make this type of coatings a good candidate for industrial applications. In the future, the substrate covered by antireflection (AR) coatings can be designed as a sensitive sensor in THz spectroscopy systems.

2. Theoretical model

When THz pulses propagates through the interfaces between two media covered by a thin metallic film, there is a theoretical description for electromagnetic waves propagating through such interfaces [17]. If the thickness d of the thin conducting film is smaller than the skin depth δ_0 ($d << \delta_0$), dispersion of electromagnetic waves through the film is negligible [18–20]. In the terahertz frequency range, the conductivity of most metals has the real part $\tilde{\sigma}_r$ of frequency independence with a negligible imaginary component $\tilde{\sigma}_i$ [21,22].

Figure 1(a) shows the coated substrate was covered by a metallic antireflection coating. The optimal impedance matching at air-film-substrate interface was achieved by changing the thickness of metallic films, so that the reflection R_{air} at the substrate-film-air interface is suppressed, i.e., the reflection coefficients r are equal to zero. Figure 1(b) shows the sample (liquids or biological samples) was placed on the coated substrate. The complex refractive index of the sample cause the impedance mismatch at sample-film-substrate interface, so that the reflection R_{sam} at the interface exists, i.e., the reflection coefficients r are not equal to zero.

Optics EXPRESS

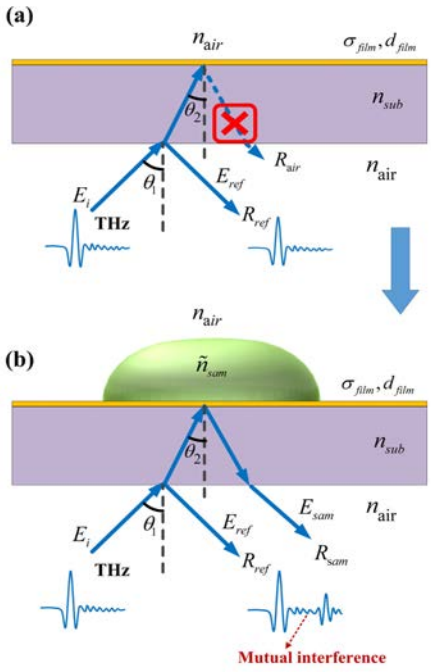

Fig. 1. Schematic of THz pulses propagating through the interfaces between two media covered by a metallic antireflection coating.

In the THz-TDs measurement of the sample on the coated substrate, the measured electric field $E_{ref+sam}(t)$ was from superposed reflections $R_{ref}+R_{sam}$, as shown in Fig. 1(b). The $E_{ref+sam}(t)$ was expressed as $E_{ref+sam}(t)=E_{ref}(t)+E_{sam}(t)$, where $E_{ref}(t)$ and $E_{sam}(t)$ were the electric fields of the THz pulses R_{ref} and R_{sam}, respectively. $E_{ref}(t)$ was measured from the coated silicon substrate, as shown in Fig. 1(a). Thus, $E_{sam}(t)$ was obtained by $E_{sam}(t)=E_{ref+sam}(t)-E_{ref}(t)$. The Fourier transformation of $E_{ref}(t)$ and $E_{sam}(t)$ were written as $E_{ref}(\omega)$ and $E_{sam}(\omega)$, respectively. According to THz pulses propagating through the interfaces in Fig. 1, $E_{sam}(\omega)$ and $E_{ref}(\omega)$ were expressed as

$$E_{sam}(\omega)=E_i(\omega)\cdot t_{air/sub}\cdot r_{sub/film/sam}\cdot t_{sub/air}\cdot\exp\left(i\cdot\frac{\omega}{c}\cdot\frac{2\cdot n_{sub}\cdot d_{sub}}{\cos\theta_2}\right) \quad (1)$$

and

$$E_{ref}(\omega)=E_i(\omega)\cdot r_{air/sub}, \quad (2)$$

where $E_i(\omega)$ is the electric field of incident THz wave, $t_{air/sub}$ is the transmission coefficient at the air-substrate interface, $r_{sub/film/sam}$ is the reflection coefficient at the substrate-film-air interface, $t_{sub/air}$ is the transmission coefficient at the substrate-air interface, $r_{air/sub}$ is the reflection coefficient at the air-substrate interface, ω is angular frequency, c is velocity of light, n_{sub} is the refractive index of the substrate, d_{sub} is the thickness of the substrate and θ_2 is incident angle of THz waves in the substrate. Thus, the ratio of $E_{sam}(\omega)$ to $E_{ref}(\omega)$ can be written as

Optics EXPRESS

$$\frac{E_{sam}(\omega)}{E_{ref}(\omega)} = \frac{t_{air/sub} \cdot r_{sub/film/sam} \cdot t_{sub/air}}{r_{air/sub}} \cdot \exp\left(i \cdot \frac{\omega}{c} \cdot \frac{2 \cdot n_{sub} \cdot d_{sub}}{\cos\theta_2} \right). \quad (3)$$

Where $r_{air/sub} = \frac{n_{air} \cdot \cos\theta_1 - n_{sub} \cdot \cos\theta_2}{n_{air} \cdot \cos\theta_1 + n_{sub} \cdot \cos\theta_2}$, $r_{sub/film/sam} = \frac{n_{sub} \cdot \cos\theta_2 - \tilde{n}_{sam} \cdot \cos\theta_1 - Z_0 \cdot \sigma_{film} \cdot d_{film}}{n_{sub} \cdot \cos\theta_2 + \tilde{n}_{sam} \cdot \cos\theta_1 + Z_0 \cdot \sigma_{film} \cdot d_{film}}$, $t_{air/sub} = \frac{2 \cdot n_{air} \cdot \cos\theta_1}{n_{air} \cdot \cos\theta_1 + n_{sub} \cdot \cos\theta_2}$ and $t_{sub/air} = \frac{2 \cdot n_{sub} \cdot \cos\theta_2}{n_{air} \cdot \cos\theta_1 + n_{sub} \cdot \cos\theta_2}$ in the S-polarization mode (the electric field is perpendicular to the plane of incidence). Here, Z_0 is the impedance of free space, θ_1 is incident angle of THz waves in air, θ_2 is incident angle of THz waves in the substrate, n_{air} is the refractive index of air, n_{sub} is the refractive index of the substrate, $\tilde{n}_{sam}$ is the complex refractive index of the sample, σ_{film} is the conductivity of the metallic films, d_{film} is the thickness of the metallic films. Similarly, the reflection and transmission coefficients for P-polarization mode (the electric field is parallel to the plane of incidence) is described in the reference [19].

In term of the above equations, the sample information was extracted from the ratio of $E_{sam}(\omega)$ to $E_{ref}(\omega)$ according to Fresnel theory. More details about the calculation procedure can be found in the literatures [8,10].

3. Experimental setup

High-resistivity (HR) silicon ($>3000\,\Omega\cdot\mathrm{cm}$) with 0.5 mm thickness was chosen as substrate. Due to negligible absorption of high-resistivity silicon in the THz frequency range, the imaginary part of refractive index of the high-resistivity silicon is negligible [23]. The HR silicon substrates can reduce the effect of material dispersion on experimental results in THz-TDs measurement [20]. The TaN films used as AR coating in this paper were prepared by RF magnetron sputtering. The sheet resistances of thin films were determined by a four-probe measurement. According to the antireflection theoretical model [20,24], the matching sheet resistance of the thin film in the impedance matching can be obtained by the theoretical calculation. Hereby, in the experiment, we need to prepare the thin films achieving the matching sheet resistance. Thus, the thickness of the thin film in the impedance matching is measured by a surface profiler. The liquid sample on the coated substrate was measured by using a terahertz time-domain spectroscopy (THz-TDs). The THz-TDs was performed in reflection mode. Photoconductor antenna illuminated by ultra-short laser pulses was used for the generation and detection of THz radiation. The pumping laser provided the pulses of 780 nm center wavelength, 100 fs pulse duration and 100 mW output power at a pulse repetition rate of approximately 80 MHz. The parabolic off-axis focusing mirrors were used to focus the terahertz beam on the sample. The frequency bandwidth in the terahertz system was limited to 1.5 THz. Outside this frequency range, the signal was too weak to obtain an acceptable signal-to-noise ratio in the terahertz system. In the THz reflection measurement, the terahertz beam was focus on the sample (incidence angle $\theta_1 = 30^\circ$) in the S-polarization mode (the electric field is perpendicular to the plane of incidence).

Optics EXPRESS

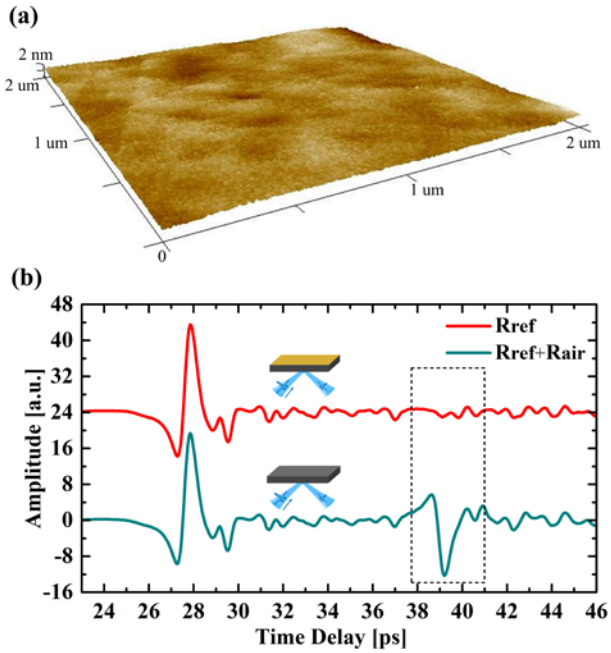

Fig. 2. AFM image of a TaN film produced by RF magnetron sputtering onto the silicon substrate (a); The main and the second terahertz pulses transmitted through bare silicon substrate and the silicon substrate with ultrathin TaN film in reflection geometry respectively (b).

4. Results and discussion

In the optimal impedance matching, the thickness of TaN films was about 14 nm. Figure 2(a) shows the AFM image of the TaN film produced by RF magnetron sputtering onto the silicon substrate. In the reflection measurements of bare substrate and coated substrate, the measured signal reflected from the bare substrate consists of several THz pulses (dark cyan curve), as shown in Fig. 2(b). The main pulse is reflected from the front side of the bare substrate, and the secondary pulse is reflected from the back side of the bare substrate. For the coated substrate, the second pulse (red curve) are completely suppressed compared with that of the bare substrate, as shown in Fig. 2(b). For the experiment of the AR self-reference method, water as the sample was measured. Firstly, air on the coated silicon substrate was used for measuring the reference refection R_{ref} (as reference) from air-substrate interface, and the reflection R_{air} at the substrate-film-air interface is suppressed, as shown in Fig. 1(a). The time-domain waveforms of the reference refection R_{ref} from air-substrate interface are shown in Fig. 3. Then, the water sample on the coated silicon was measured, and the time-domain waveforms of the measured superposed reflections $R_{ref} + R_{sam}$ from both interfaces are shown in Fig. 3. In the experiment, the coated substrate was placed on the stage by the holder, so the misplacement error from the coated substrate was avoided. These THz measurements were repeatedly performed for three times, to ensure accuracy of the experimental results.

Optics EXPRESS

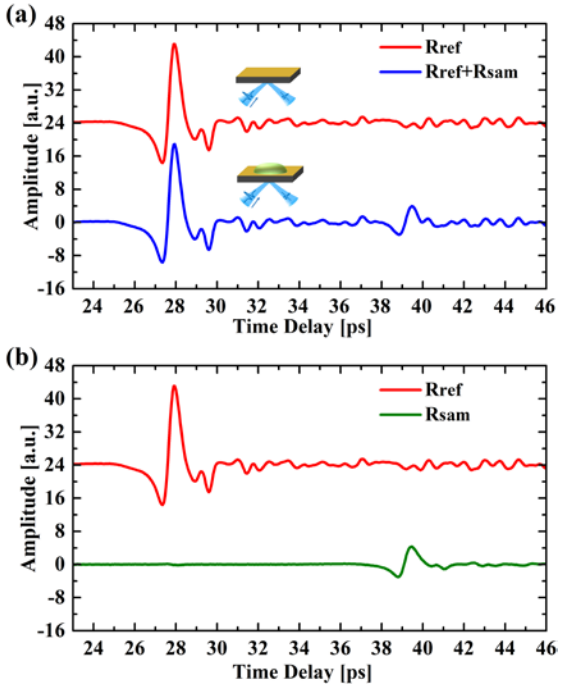

Fig. 3. Time domain waveforms of the measured reference reflection R_{ref}, the measured superposed reflection $R_{ref}+R_{sam}$ and recovered sample reflection R_{sam} using our proposed method.

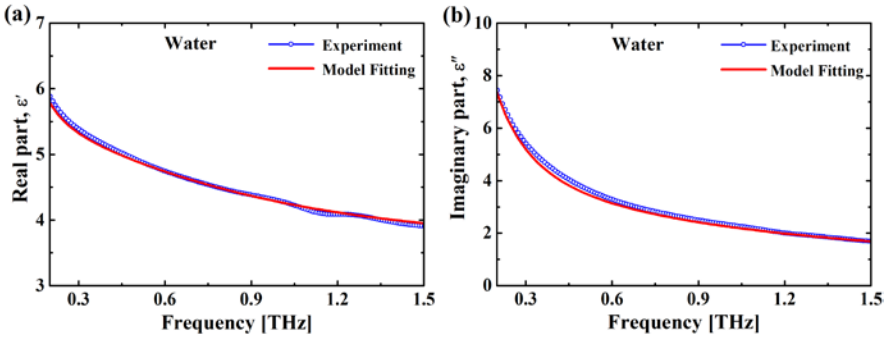

Fig. 4. The real and imaginary part of the dielectric function of water from the experiment and Debye model fitting.

Figure 3 shows the time-domain waveforms of the superposed reflections $R_{ref}+R_{sam}$ from both interfaces. The mutual interference caused by the ring tail of the reference reflection was obvious. The sample reflection R_{sam} from the substrate-film-water interface was accurately recovered using the AR self-reference method, as shown in Fig. 3. In order to compare our results with published data, the dielectric functions of the water were obtained using the aforementioned theory, and the dielectric spectrum of water was shown in Fig. 4. The real and imaginary parts of the dielectric function are written as $\tilde{\varepsilon}_r = \varepsilon' - i\varepsilon'' = (n - i\kappa)^2$. The dielectric spectrum of water was analyzed using the double Debye model with two relaxation times τ_1 and τ_2 [13, 25, 26],

Optics EXPRESS

$$\tilde{\varepsilon}_r(\omega) = \varepsilon_\infty + \frac{\varepsilon_s - \varepsilon_m}{1 + i\omega\tau_1} + \frac{\varepsilon_m - \varepsilon_\infty}{1 + i\omega\tau_2} \quad (4)$$

In Table 1, we compare the fitting parameters obtained using the experiment results with the data from the literature [8, 13, 20–22]. The results of our analysis are in a good agreement with the values of the Debye parameters published in the literatures [10, 13, 25–27]. This demonstrates that the AR self-reference method can precisely characterize the dielectric properties of liquid samples. The small fluctuation of the dielectric spectrum was mainly caused by residual water vapor in the THz beam path. The residual water vapor has an effect on the dielectric spectrum of the testing liquid. As a result, using AR self-reference method, the superposed reflection interfering with the sample reflection was well eliminated, and the sample reflection from the substrate-film-sample interface was accurately recovered, as shown in Fig. 3. Figure 5 depicts the potential application of auto-measurement spectroscopy systems using the self-reference method. Therefore, the AR self-reference method can eliminate mutual interference and improve the THz measurements of liquid and biological samples.

Table 1. Parameters of double Debye model of water

	ε_s	ε_∞	ε_m	τ_1 (ps)	τ_2 (ps)
This work	78.8	3.5	5.2	8.3	0.18
Jepsen *et al.* [10]	78.4	3.5	5.2	7.9	0.18
Rønne *et al.* [13]	80.2	3.3	5.2	8.5	0.17
Barthel *et al.* [27]	78.4	4.5	6.2	8.3	1.02
Pickwell *et al.* [25]	78.8	4.1	6.6	10.6	0.18
Kindt *et al* [26].	78.4	3.5	4.9	8.2	0.18

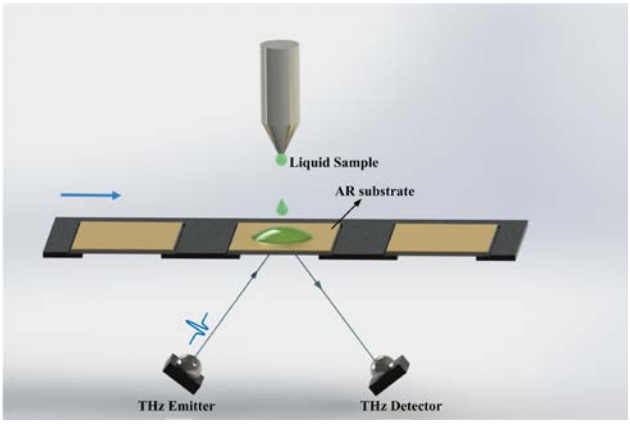

Fig. 5. Application of auto-measurement spectroscopy systems using the self-reference method.

5. Conclusions

In conclusion, we have described a theoretical model for the AR self-reference method based on the ultra-thin metallic films, which was validated with experimental determination of the dielectric function of water. The ultra-thin TaN nanofilms can be used as an efficient broadband AR coating in the terahertz frequency range. Moreover, we validated that the data

Optics EXPRESS

extracted from water sample were in a good agreement with the values of the Debye parameters reported in the literature. We have shown the AR self-reference method can completely eliminate mutual interference, accurately recover the sample reflection and efficiently improve the THz measurement for liquid and biological samples. The AR self-reference method provides a promising route for THz spectroscopy sensors in the terahertz application, and makes it attractive to commercial applications.

Funding

The Fund from Hefei University of Technology (407-0371000019); Sichuan Province Science and Technology Support Program (No. 2016GZ0250); the Fundamental Research Funds for the Central Universities (Grant No. JD2017JGPY0006); National Natural Science Foundation of China (Grant No.51607050); MINECO (MAT2015–74381-JIN to B.P., RYC-2014–16962 and CTQ2017-89588-R to P.dP.); Xunta de Galicia (Centro singular de investigación de Galicia accreditation 2016–2019, ED431G/09); European Union (European Regional Development Fund – ERDF).